

LED-LED PORTABLE OXYGEN GAS SENSOR

I.M. Perez de Vargas-Sansalvador^a, C. Fay^b, M.D. Fernandez-Ramos^a, D. Diamond^b, F. Benito-Lopez^b, L.F. Capitan-Vallvey^{a}*

^aDepartment of Analytical Chemistry, Faculty of Sciences, Campus Fuentenueva, University of Granada, E-18071, Granada, Spain.

^bCLARITY: Centre for Sensor Web Technologies, National Centre for Sensor Research, Dublin City University, Dublin 9, Ireland.

Abstract

A portable instrument for oxygen determination, based on the quenching of phosphorescent octaethylporphyrin by gaseous O₂ has been developed using the fluorimetric paired emitter–detector diode technique (FPEDD). The instrument configuration consists of two light emitting diodes (LEDs) facing each other including an interchangeable support containing a phosphorescent membrane in between, in which one of the LEDs is used as the light source (emitter LED) and the other working in reverse bias mode as the light detector. The feasibility of using a LED as a luminescent detector is studied. Its small size allows the integration of the instrument into a portable measurement system. A systematic study of the system capabilities as a portable instrument, was carried out in order to optimize: range, sensitivity, short term and long term stability, dynamical behaviour, temperature influence, humidity influence and temporal drift.

Keywords: Oxygen sensor, Gas sensor, Optical sensor, Paired emitter detector-diode sensor; Portable instrumentation.

Introduction

One of the current trends in analytical chemistry is the development of portable instrumentation, with characteristics of robustness, compactness, small size, and the capability of delivering sensory information anywhere is required. In this approach, special attention is paid to the use of LEDs as near monochromatic low power sources of light. On the other hand, LEDs as detectors are attractive due to the reduction of electronic component complexity by eliminating the need for wavelength selection (*e.g.* photodiodes) if the absorption spectrum of the analyte or its derivative is compatible with the emission spectrum of the selected emitter LED [1].

It has been established that the internal photoelectric effect (opposite to electroluminescence phenomena, enabling the conversion of electric energy into light by LED) allows the use of an LED as a light detector when it is operated in the reversed mode [2;3].

The Paired Emitter-Detector Diode (PEDD)-based photometry technique is more developed, is well developed nowadays, where a complete absorbance detector can be easily constructed using only two LEDs [1;4]. In such an instrument, one of them (the LED-emitter) compatible with the absorption spectrum of analyte or a derivative, whereas the second one (the LED-detector) plays the role of detector of non absorbed radiation. The integration of such compatible LEDs leads to the construction of compact PEDD-based instruments which are useful as dedicated and complete photometers.[ref Isabel]

The first application of a PEDD system was made to measure colour, and to monitor colorimetric chemical reactions (pH induced colour change) [5] or to colorimetrically detect cadmium(II) and lead(II) in water samples [6]. Moreover, this sensing approach can be arranged to make transmission or reflectance measurements [4], so it was possible to monitor color variations due to pH in flow systems [7] or phosphate determination [8], the detection of dyes and metal ions [9], automated acid–base titrations [10], kinetic measurements performed directly inside flow-through reaction chambers [11] and open-tubular bioreactors [12], as well as enzyme activity assays performed in flow injection analysis (FIA) format [13]. Flow-through PEDD sensors for redox species based on prussian blue films [14] as well as PEDD-based sensors for gaseous acidic species [15] and carbon dioxide [16], all based on membranes containing immobilized pH-indicators, have been developed. Only recently, a redox optosensor, which has a polyester film with prussian blue and glucose oxidase co-

immobilized working simultaneously as a chemo- and bioreceptor, has been applied for PEDD-based glucose biosensor development [17]. The further integration of PEDDs with optosensing membranes allows the development of complete absorption-based sensors [16]. Moreover, by coupling with chromatographic techniques, PEDDs have been applied for the detection of some species like Mn(II)- and Co(II)-2-(pyridylazo)resorcinol complexes and alkaline earth metals in water solutions [18-20].

Fluorimetry is another important field of analytical chemistry where LEDs are intensively investigated, since it was found that LED induced fluorescence (LED-IF) can be useful for analytical purposes [21;22]. LED-IF based systems are widely reported in the analytical literature [23-28], however the main attention is put into the improvement of fluorescence excitation efficiency, for instance by changing LED-emitter geometry.

The first reported study regarding the use of LEDs applied as a detector for fluorescence was a tri-LED-based system for the determination of quinine in tonics where a cuvette holder with mounted LEDs allowed for dual, photometric and fluorimetric detection of analytes [29]. Recently, it was demonstrated that fluorimetric detectors made of two appropriate LEDs can be applied to do measurements in continuous flow [30]. These flow-through prototypes of fluorimetric PEDDs (FPEDDs) enable the determination of fluorescent analytes at low concentration levels [31]. In order to get an effective luminescence excitation, the emission spectrum of LED emitter should be compatible with the excitation spectrum of the analyte or recognition system plus the LED detector should produce radiation of lower energy than measured fluorescence [30].

The cost of monitoring gases is of major concern for environmental applications [C. Fay, *Sensors* **2011**, *11*, 6603-6628], therefore instrumentation, designed using low cost components like LEDs, ensures high production at low costs. This instrumentation can be widely used by the environmental agencies in more locations more often, promoting a better and more realistic environmental monitoring and control. In addition, portable instruments capable of measuring gas concentrations, *e.g.* oxygen, carbon dioxide, methane, etc, offer the possibility of measuring on the point-of-site or even in a wearable personalised configuration, *e.g.* fire-fighters and doctors. [Radu T, World Academy of Science, Engineering & Technology; Oct2009, Vol. 58, p80-83, 4p]

Moreover gas ration and flow control are of crucial importance in the sanitary sector [Stuart-Andrews, *C. British Journal Of Anaesthesia* **2007**, *98*, 45-52]. Instrumentation

capable of achieving accurate measurements of certain gases, *e.g.* oxygen, on the point of side will speed up the response of the sanitary authorities, nurses or doctors, in case of an unexpected event and therefore reduce fatalities and sanitary costs. The main goal of this study is the development of a portable device integrating a luminescence paired emitter–detector diode system for the determination of a gaseous analyte, oxygen, based on the luminescence quenching of a sensing film containing the dye platinum octaethylporphyrin complex immobilized in a polystyrene membrane [32].

Experimental

Chemical and reagents and equipment

The reagents used were platinum octaethylporphyrin complex (PtOEP, Porphyrin Products Inc., Logan, UT, USA) and 1,4-diazabicyclo[2.2.2]octane (DABCO; 98%, from Sigma–Aldrich Química S.A., Madrid, Spain). The polymer and solvent used were tetrahydrofuran (THF) and polystyrene (PS, average MW 280,000, T_g: 100 °C, GPC grade) both from Sigma. The cocktail was prepared by weighing the chemicals with a precision of ±0.01 mg in a DV215CD balance (Ohaus Co., Pine Brook, NJ, USA). The gases O₂ and N₂ used were of a high purity (>99%) and were supplied in gas cylinders by Air Liquid S.A. (Madrid, Spain).

The standard mixtures of oxygen were produced using nitrogen as the inert gas component by controlling the flow rates of oxygen and nitrogen gases entering a mixing chamber using a computer-controlled mass flow controller (Air Liquid Spain S.A., Madrid, Spain) operating at a total pressure of ~~760 Torr~~ 1 atm and a flow rate of 500 cm³ min⁻¹.

The interchangeable membrane platform was fabricated using a laser ablation system–excimer/CO₂ laser, Optec Laser Micromachining Systems, Belgium and a laminator system Titan-110, GBC, USA. 150 μm PMMA (poly(methylmethacrylate)) sheets were purchased from Goodfellow Cambridge Ltd, UK; 50 μm double-sided pressure sensitive adhesive film (AR8890) was obtained from Adhesives Research, Ireland and Mylar-type polyester from Goodfellow Cambridge Ltd, UK.

The red LEDs used were supplied by Digi-Key (Ireland Part No. 67-1612-ND) and the green LEDs, L-7113GC were supplied by Kingbright manufacture (Radionics, 451-6537).

Instrumentation

Figure 1 presents a diagram of the system setup used showing a custom designed (using a CAD package) and fabricated frame support. The purpose of this design was to constrain the movements of each component during experimentation and therefore to eliminate errors that may arise from mechanical layout. It can be seen that both LEDs were fixed and also that the frame design incorporated two slits for modularity *i.e.* for interchangeability of the membrane.

Figure 1

Figure 2 presents a schematic representing the relevant electronic implementation of the system. At the heart of the instrument was the microcontroller (MSP430 F449) which was responsible for complete system operation *i.e.* measurement, actuation of the emitter LED, timing and communications to the PC. Initially, the microcontroller was programmed to firstly charge the detector LED *i.e.* the IO was set to output mode and then to logic high (3.3 V). Next, in the same manner (*i.e.* by setting the emitter IO to logic high), power was supplied to the emitter LED via the transistor. After that, the detector LED's IO was set to input mode where its logic level was checked 65535 (2¹⁶ -1) times and subsequently incremented a software counter if the logic level was 1. Once complete, the emitter LED was switched off and the resulting counter value was communicated to a PC over the microcontrollers UART port and captured using a communications package (HyperTerminal, Microsoft). Based on the kinetics of the chemistry involved during development and through previous studies (see Figure 2), the measurement and reporting regime was set to repeat without end at a frequency of 1 Hz.

Figure 2

Sensing interchangeable membranes preparation

In order to carry out the design of an easy to handle instrument, the membranes were cast on a Mylar support. . This allows an easy interchange of the membrane when, for instance, testing different systems and to reduce stress during the storage process too. Since the membrane support is designed by AutoCAD, making them reproducible from one membrane to another, the overall instrument accuracy is improved. Also the membrane

holder always guarantee the same position of the membrane in the holder, what is an improvement compare with casting the membrane on top of the LEDs.

Mixtures for the preparation of the oxygen-sensitive membrane were made by dissolving 0.5 mg of PtOEP and 12 mg of DABCO in 1 mL of a solution of 5% (w/v) of PS in freshly distilled THF. The sensitive membranes were cast by placing 10 μL of the cocktail on the Mylar interchangeable membrane with the aid of a micropipette. After the addition, the membrane was left to dry in darkness in a THF atmosphere for 1 hour. The obtained transparent pink membrane was homogeneous with an estimated average thickness of about 75 μm and a PtOEP concentration of 0.055 mol kg^{-1} polymer. Oxygen-sensing membranes need to be cured in darkness for 9 days before use [33]. The prepared membranes were kept inside a box in darkness when they were not in use.

Measurement conditions

The standard mixtures for instrument calibration and characterisation (O_2 in N_2) were produced using N_2 as the inert gas component and by controlling the flow rates of the different high purity gases ($\geq 99.5\%$) N_2 and O_2 , in each case, entering a mixing chamber using a computer-controlled mass flow controller operating at a total pressure of 1 atm and a flow rate of 500 $\text{cm}^3 \text{min}^{-1}$, with a specified accuracy of $\pm 0.5\%$ of the reading and $\pm 0.1\%$ of full scale. For the portable instrument characterisation, the measurements were performed after 2 min equilibration of the instrument atmosphere with the gas mixtures obtained with the gas blender indicated above.

In order to produce different humidity conditions, a controlled evaporator and mixer (CEM) system (Bronkhorst high-tech B.V., AK Ruurlo) was used. This system consists of a mass flow controller for measurement and control of the carrier gas flow (N_2), a Coriflow which allows the measurement of mass flow for liquids (water in this case) and a CEM 3-way mixing valve and evaporator for control of the liquid source flow and mixing the liquid with the carrier gas flow resulting in total evaporation. In addition a temperature controlled heat-exchanger was employed to produce a complete evaporation of the liquid, and allows preparing mixtures with relative humidity (RH) between 0 and 100%.

All measurements were repeated six times in total in order to check for experimental error. A homemade thermostatic chamber, with a lateral hole for the connexion to a computer

and gas tubing entrance, made possible to maintain a controlled temperature between $-50\text{ }^{\circ}\text{C}$ and $50\text{ }^{\circ}\text{C}$ with an accuracy of $\pm 0.5\text{ }^{\circ}\text{C}$, for the thermal characterisation of the sensor.

Results and discussion

Optical response of sensing membranes and instrument response

The mechanism of the response of the instrument is based on the dynamic quenching of the PtOEP complex luminescence emission caused by oxygen that results in changes of both, luminescence intensity and lifetime. Another gas of interest that can be analysed using this mechanism is carbon dioxide [ref Isabel], which in combination with oxygen, are of high clinical interest in air pressure masks and gases on blood, among others.

As shown in Figure 3, this compound had a maximum of absorption at around 537 nm attributed to the metalloporphyrin Q-band. The sensing membrane containing this substance is excited by a red LED (maximum at 525 nm) which emission overlaps with the excitation wavelength (537 nm) of the luminescence substance. PtOEP has the maximum emission at 655 nm that overlaps with the spectrum of green LEDs that acted as the detector and shows an emission maximum at 670 nm.

Figure 3

The system presented here responded to O_2 via changes in the luminescence emission of the PtOEP which generated consequent changes in the discharge time of the reverse biased detector LED, that are related to the O_2 concentration. When increasing the O_2 concentration in the surrounding atmosphere the quantity of radiation that reaches the detector LED decreases, so the time required to discharge the luminescent detector LED increases. As a consequence, we can correlate the time required to discharge the luminescent detector LED to the luminescence intensity of the sensing membrane.

In order to find the optimum membrane for oxygen sensing, different amounts of the cocktail (5, 7 and 10 μL) were cast on the interchangeable support by spin coating and the difference between the discharge time at pure nitrogen (t_0) and pure oxygen (t_{100}) with each of the membranes was investigated. The best results in terms of t_0-t_{100} , that is the maximum difference between the analytical signals measured, were obtained with the higher amount of

composition tested (Figure 4) and therefore this volume was selected for preparing the sensing membranes.

Figure 4

To link discharge time and oxygen concentration the Stern–Volmer equation was used. The value I_0 corresponds to the intensity in the absence of oxygen and I at any oxygen concentration; t_0 corresponds to the discharge time in the absence of oxygen and t to the discharge time at any oxygen concentration, finally K_{SV} is the Stern-Volmer constant,

$$\frac{I_0}{I} = \frac{t_0}{t} = 1 + k_{sv}[O_2] \quad \text{Equation 1}$$

The fittings to the Stern–Volmer equation (Eq. 1) are linear for low oxygen concentrations up to 2 % of oxygen (see Fig. 5) and show a downward curvature at higher oxygen concentrations (Figure 5) according to the literature [34;35]. This curvature can be correctly fitted using an empirical function similar to a modified Stern–Volmer equation [36;37] (eq. 2, where f_1 is the fraction of sites in membrane with a Stern–Volmer quenching constant, K_{sv}) resulting in a linear function (a: 12.02; b: 1.79; coefficient of determination R^2 : 0.999).

$$\frac{I_0}{I_0 - I} = \frac{t_0}{t_0 - t} = \frac{1}{f_1 k_{sv} [O_2]} + \frac{1}{f_1} = \frac{a}{[O_2]} + b \quad \text{Equation 2}$$

Analytical characterisation

The exponential relationship between the discharge time and O_2 concentration (eq. 2) is linearized using a modified Stern–Volmer equation type. The working range of the instrument is extended up to 30% of oxygen, because at higher percentages the decreasing in the discharge time is lower, increasing the error.

The limit of detection (LOD) was calculated from the raw exponential experimental data using the first three points that can be adjusted to a straight line ($t_{discharge} = 2541.5 [O_2] + 43720$; $R^2 = 0.991$) [38], by using the conventional approach defined by $LOD = t_0^N - 3 s_0$, where t_0^N is the blank or average value in the absence of oxygen and s_0 is the critical level or

standard deviation of the blank, which was determined from six replicate measurements. The limit of quantification (LOQ) of the instrumental procedure was obtained from the calibration function by using $LOD = t^N_o + 10s_o$. The LOD found using this approach was 0.01% and the LOQ was 0.16% of O₂.

A study of the dynamic response of the sensing membrane when exposed to alternating atmospheres of pure O₂ and pure N₂ was carried out. The response time was calculated from between 10% and 90% of the maximum signal, obtaining a value of 6.75 ± 0.5 s, and the recovery time from 90% to 10% was found to be 55.0 ± 0.81 s.

In all cases, the signal changes were fully reversible and hysteresis was not observed during the measurements. The response and recovery times are lower than those obtained for other system developed by us (response time 28.5 ± 0.6 s and the recovery time 59.0 ± 2.2 s) [32].

The temporal drift of the measurements were studied by measuring at a fixed concentration of 21% oxygen for 14 hours, taking measurements every 2 seconds. The result obtained is $0.029\% \text{ h}^{-1}$ which is a reasonable value.

The precision of the proposed prototype was determined by studying the intra-day reproducibility. Seven measurements at 100% N₂ and 100% O₂ were performed using the same membrane at 15 minutes intervals with 6 replicates each. A good reproducibility with a relative standard deviation of 0.54% was obtained for t_0 - t_{100} .

As it is well known, temperature has a considerable influence on the sensitivity of luminescent sensors like PtOEP [37;39]. The thermal dependence of the sensing membranes was evaluated by acquiring the response of the instrument at temperatures between 5 °C and 30 °C. From this study, an increasing in sensitivity was observed with temperature. This non-negligible cross-sensitivity of the sensor can be attributed to a thermally activated non-radiative decay [40-43]

Figure 6

The data obtained at each temperature (Figure 6) have been modelled using eq. 2, obtaining different values for the fitting parameters a and b for each temperature. A modelling function for these fitting parameters with the temperature can be found including the thermal dependence of the oxygen sensor in these constants. In this case, an exponential function was used for both parameters. Obtaining for the first parameter ($a = 39.262e^{-0.052T}$;

$R^2 = 0.989$) and for the second parameter ($b = 2.670e^{-0.022T}$; $R^2 = 0.984$) with the temperature expressed in degrees Celsius.

In order to evaluate the possible effects that humidity may have on the measurements of the oxygen concentration, a study of the oxygen response at different humidity atmospheres (20, 30, 40, 50, 60, 70, 80, 90, 100% RH) at five different oxygen concentrations (0, 2, 10, 20 and 30% O₂) has been carried out using the climatic chamber. The percentage of variation between the biggest and the smallest value of the response of the instrument at each discrete RH level was calculated; the results showed that the variations oscillated between 0.01 and 3.5%. Because of the small difference found, it is concluded that the humidity conditions did not significantly affect the sensor performance.

Stability was studied by means of an inter-day reproducibility measuring t_0 and t_{100} (with the same membrane as in the intra-day study) for 2 months (n= 8 per day) finding a relative standard deviation of 6.91%.

Table 1 shows a comparison of the performance of the proposed instrument for O₂ with different optical sensing instrument from literature. The response time obtained with this new system is greater than two fold increase in comparison to the previous establish system, even the response and recovery times obtained here are comparable and/or lower than other sensing schemes widely used for O₂ sensing.

Besides, the proposed design is simpler than most of the comparable prototypes previously developed [44-47] where two LEDs and two photodetectors were used. A single channel sensor module was designed, mounted and tested [48], where the reference channel was removed and the signal channel synchronisation was performed by the microcontroller. The proposed design is more compact and offers better possibilities for miniaturisation in portable instrumentation.

Table 1

Conclusions

A portable instrument for oxygen monitoring has been developed and tested under different conditions of temperature and relative humidity. The system is based on a FPEDD, where two LEDs were used, one acting as the light source and the other as the light detector. The instrument was capable of measuring oxygen concentration up to 30%. This instrument

was shown to be sensitive to changes in temperature but not to relative humidity. The limit of detection was found to be 0.01% of O₂ and its response and recovery times obtained were very low, 6.75 ± 0.5 s and 55.0 ± 0.81 s, respectively.

The sensing membranes can be used for more than two months and they show a low temporal drift of 0.41 % for 14 hours.

Comparatively with other portable instrumentation for O₂ monitoring, the use of a system FPEDD offers a miniaturized form factor, good robustness, a reduced response time, and a relatively similar recovery times than existing instrumentation. These excellent characteristics, coupled with a very good design, make this instrument a promising tool to be used in portable instrumentation.

Moreover, in the future a portable instrument for measurement of both oxygen and carbon dioxide at the same time can be achieved, since both gases have been measured separately with good results.

Acknowledgements.

We acknowledge financial support from the Ministerio de Economía y Competitividad, Dirección General de Enseñanza Superior (Spain) (Projects CTQ2009-14428-C02-01 and CTQ2009-14428-C02-02) and the Junta de Andalucía P10-FQM-5974 and European Regional Development Funds. I.M.P.V.S. thanks to Junta de Andalucía for the grant “Estancias de Excelencia 3/2009” and University of Granada for “Contrato Puente”. Authors C.F., D.D. and F.B.L. acknowledge support from Science Foundation Ireland under grant 07/CE/I1147.

References

1. O'Toole M, Diamond D (2008) *Sensors* 8:2453-2479.
2. Lindsay RH, Paton BE (1976) *Am. J. Phys.* 44:188.
3. Mims FM (1992) *Appl. Opt.* 31:6965-6967 .
4. Lau K-T, Baldwin S, O'Toole M, Shepherd R, Yerazunis WJ, Izuo S, Ueyama S, Diamond D (2006) *Anal. Chim. Acta* 557:111-116.
5. Lau KT, Baldwin S, Shepherd RL, Dietz PH, Yerzunis W, Diamond D (2004) *Talanta* 63:167-173.

6. Lau KT, McHugh E, Baldwin S, Diamond D (2006) *Anal. Chim. Acta* 569:221-226.
7. O'Toole M, Lau KT, Diamond D (2005) *Talanta* 66:1340-1344.
8. O'Toole M, Lau KT, Shepherd R, Slater C, Diamond D (2007) *Anal. Chim. Acta* 597:290-294.
9. Tymecki L, Pokrzywnicka M, Koncki R (2008) *Analyst* 133:1501-1504.
10. da Silva MB, Crispino CC, Reis BF (2010) *J. Braz. Chem. Soc.* 21:1854-1860.
11. Koronkiewicz S, Kalinowski S (2011) *Talanta* 86:436-441.
12. Rozum B, Gajownik K, Tymecki L, Koncki R (2010) *Anal. Biochem.* 400:151-153.
13. Tymecki L, Brodacka L, Rozum B, Koncki R (2009) *Analyst* 134:1333-1337.
14. Pokrzywnicka M, Cocovi-Solberg D, Miro M, Cerdá V, Koncki R, Tymecki L (2011) *Anal. Bioanal. Chem.* 399:1381-1387.
15. Orpen D, Beirne S, Fay C, Lau KT, Corcoran B, Diamond D (2011) *Sens. Actuators B* 153:182-187.
16. Perez de Vargas-Sansalvador IM, Fay C, Phelan T, Fernandez-Ramos MD, Capitán-Vallvey LF, Diamond D, Benito-Lopez F (2011) *Anal. Chim. Acta* 699:216-222.
17. Cocovi-Solberg DJ, Miro M, Cerdá V, Pokrzywnicka M, Tymecki L, Koncki R (2012) *Talanta* [doi:10.1016/j.talanta.2011.11.021](https://doi.org/10.1016/j.talanta.2011.11.021).
18. Barron L, Nesterenko PN, Diamond D, O'Toole M, Lau KT, Paull B (2006) *Anal. Chim. Acta* 577:32-37.
19. O'Toole M, Lau KT, Shazmann B, Shepherd R, Nesterenko PN, Paull B, Diamond D (2006) *Analyst* 131:938-943.
20. O'Toole M, Barron L, Shepherd R, Paull B, Nesterenko P, Diamond D (2009) *Analyst* 134:124-130.
21. Cho EJ, Bright FV (2001) *Anal. Chem.* 73:3289-3293.
22. Dasgupta PK, Eom IY, Morris KJ, Li J (2003) *Anal. Chim. Acta* 500:337-364.
23. Götz S, Karst U (2007) *Anal. Bioanal. Chem.* 387:183-192.
24. Hauser PC, Tan SSS (1993) *Analyst* 118:991-995.
25. Hart SJ, Ji Ji RD (2002) *Analyst* 127:1693-1699.
26. Hart SJ, Ji Ji RD (2002) *Analyst* 127:1693-1699.
27. de Jong EP, Lucy CA (2006) *Analyst* 131:664-669.

28. Yang FB, Pan JZ, Zhang T, Fang Q (2009) *Talanta* 78:1155-1158.
29. Pokrzywnicka M, Koncki R, Tymecki L (2010) *Talanta* 82:422-425.
30. Tymecki L, Pokrzywnicka M, Koncki R (2011) *Analyst* 136:73-76.
31. Tymecki L, Rejnis M, Pokrzywnicka M, Strzelak K, Koncki R (2012) *Anal. Chim. Acta* 721:92-96.
32. Capitán-Vallvey LF, Asensio LJ, Lopez-Gonzalez J, Fernandez-Ramos MD, Palma AJ (2007) *Anal. Chim. Acta* 583:166-173.
33. Perez de Vargas-Sansalvador IM, Carvajal MA, Roldan-Muñoz OM, Banqueri J, Fernandez-Ramos MD, Capitán-Vallvey LF (2009) *Anal. Chim. Acta* 655:66-74.
34. Douglas P, Eaton K (2002) *Sens. Actuators B* 82:200-208.
35. Lee SK, Okura I (1998) *Spectrochim. Acta A* 54:91-100.
36. Carraway ER, Demas JN, De Graff BA, Bacon JR (1991) *Anal. Chem.* 63:337-342.
37. Demas JN, DeGraff BA, Xu W (1995) *Anal. Chem.* 67:1377-1380.
38. ISO (2008) ISO 11843-5:2008. Capability of Detection. Part 5: Methodology in the linear and non-linear calibration cases. International Standardization Organization, Geneva.
39. Schanze KS, Carroll BF, Korotkevitch S, Morris MJ (1997) *AIAA J.* 35:306-310.
40. Lee SK, Okura I (1997) *Anal. Sci.* 13:535-540.
41. Lupton JM, Klein J (2002) *Chem. Phys. Lett.* 363:204-210.
42. Tsuboi T, Murayama H, Penzkofer A (2006) *Thin Sol. Films* 499:306-312.
43. Martínez-Olmos A, de Vargas-Sansalvador IMP, Palma AJ, Banqueri J, Fernandez-Ramos MD, Capitán-Vallvey LF (2011) *Sens. Actuators B* 160:52-58.
44. Hauser PC (1995) *Meas. Sci. Technol.* 6:1081-1085.
45. Papkovsky DB, Ponomarev GV, Ogurtsov V, Dvornikov AA (1993) *SPIE Vol. 2085 Biochemical and Medical Sensors* 54-60.
46. Trettnak W, Gruber W, Reininger F, Klimant I (1995) *Sens. Actuators B* 29:219-225.
47. Trettnak W, Kolle C, Reininger F, Dolezal C, O'Leary P (1996) *Sens. Actuators B* 35-36:506-512.
48. Palma AJ, López-González J, Asensio LJ, Fernandez-Ramos MD, Capitán-Vallvey LF (2007) *Sens. Actuators B* 121:629-638.
49. Trinkel M, Trettnak W, Kolle C (2000) *Quim. Anal.* 19:112-117.

50. Costa-Fernandez JM, Bordel N, Campo JC, Ferrero FJ, Perez MA, Sanz-Medel A (2000) *Mikrochim. Acta* 134:145-152.
51. McGaughey O, Nooney R, McEvoy AK, McDonagh C, MacCraith BD (2005) *Proc. SPIE-Int. Soc. Opt. Eng.* 5993:59930R-1-59930R/12.
52. Perez de Vargas-Sansalvador IM, Martinez-Olmos A, Palma AJ, Fernandez-Ramos MD, Capitán-Vallvey LF (2011) *Mikrochim. Acta* 172:455-464.
53. Cai Y, Shinar R, Zhou Z, Shinar J (2008) *Sens. Actuators B* 134:727-735.

Table 1. Comparison of performance of proposed instrument for O₂ with different optical O₂ sensing instruments in literature.

Technique	Range	LOD	Precision	Remarks	Reference
Fluorimetry	< 100 vpm	–	–	Phase modulation- based instrument	[49]
Fluorimetry	<7.8 ppm	0.11 ppm	5.9 %	Lifetime-based FO instrument	[50]
Fluorimetry/Multianalyte	<50%	–	–	Platform for indoor-air quality	[51]
Phosphorimetry	< 21%	0.16% v/v	5.60%	Flow-through FO RTP lifetime sensor RTP lifetime sensor	[50]
Phosphorimetry	<30%	–	0.2-0.4%	Coated PD	[32]
Phosphorimetry/Multianalyte	<30%	0.01%	0.05%	Coated LED and PD	[52]
Photoluminescence/Multianalyte	–	–	–	Alq3OLEDs/PtOEP-film, Organic light-emitting instruments (OLEDs)	[53]
Photoluminescence/Multianalyte	<30%	0.14%	0.07%	Coated LED and PD	[43]
Fluorimetry	<30%	0.01%	0.05%	FPEDD technique	Current study

Figures

Figure 1. Diagram showing the layout of the Emitter LED, Detector LED and the interchangeable membrane within the custom made support frame.

Figure 2. Electronic schematic showing the relevant circuitry and interconnects between the Power Source, Controller Board, Emitter and Detector LED components.

Figure 3. Excitation and emission spectra. A) Excitation spectrum of PtOEP; B) Emission spectrum of red LED; C) Emission spectrum of PtOEP; D) Emission spectrum of green LED.

Figure 4. Discharge time *versus* time for membranes with different amount of the sensing composition. Membrane 1: 5 μL ; membrane 2: 7 μL ; and membrane 3: 10 μL .

Figure 5. A) Response of the system. Discharge time *versus* oxygen concentration. B) Linearisation first three points of the experimental raw data for the calculation of the LOD and LOQ.

Figure 6. Temperature effect on the instrument response from 5 to 30°C

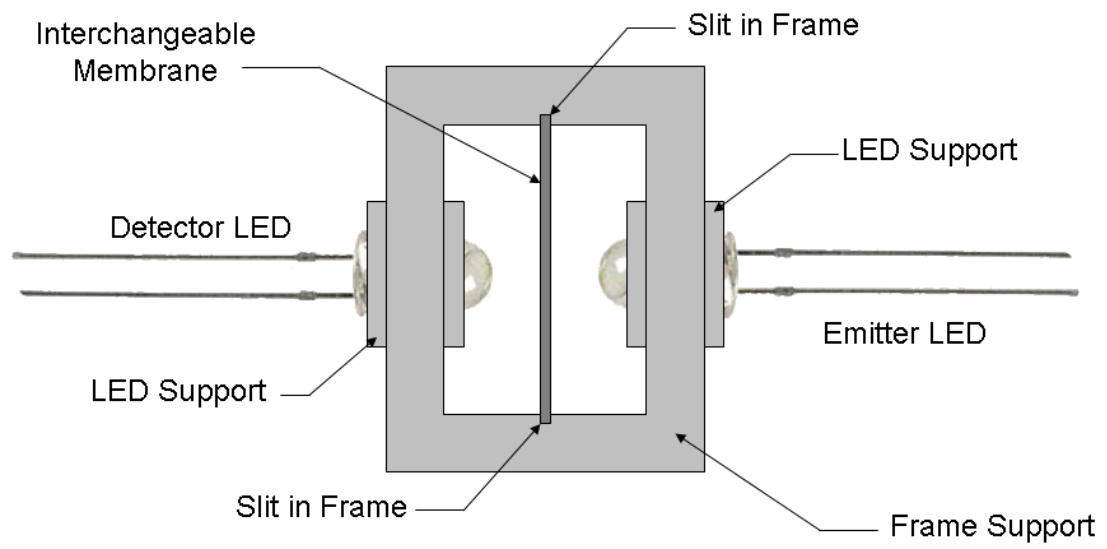


Figure 1

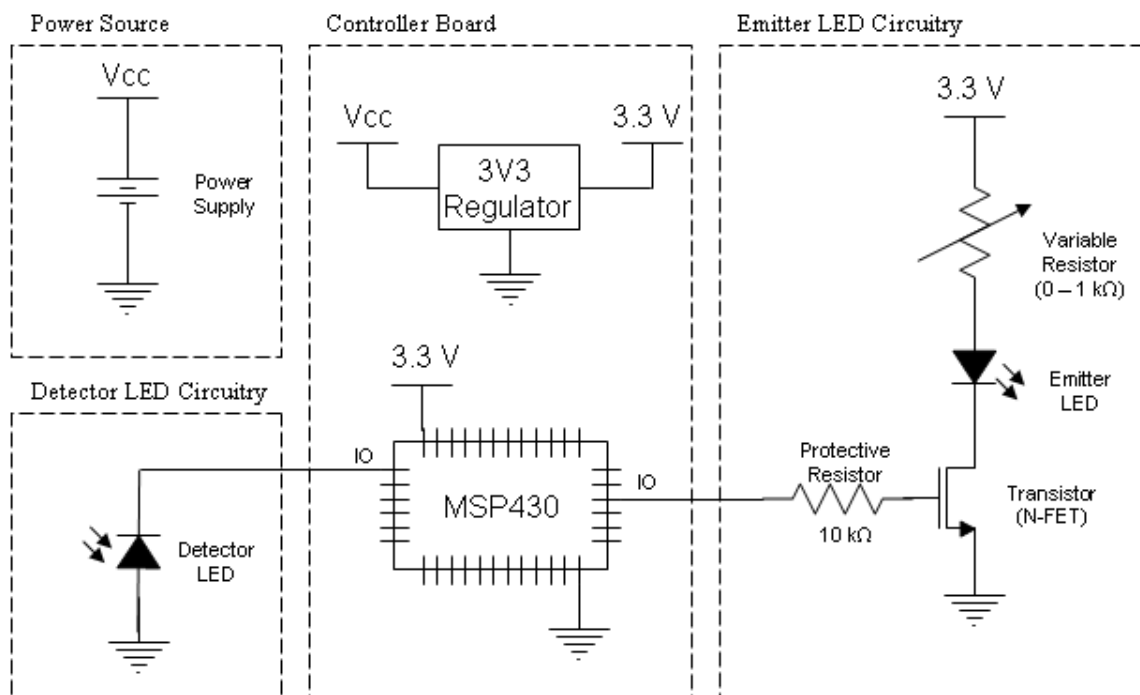


Figure 2

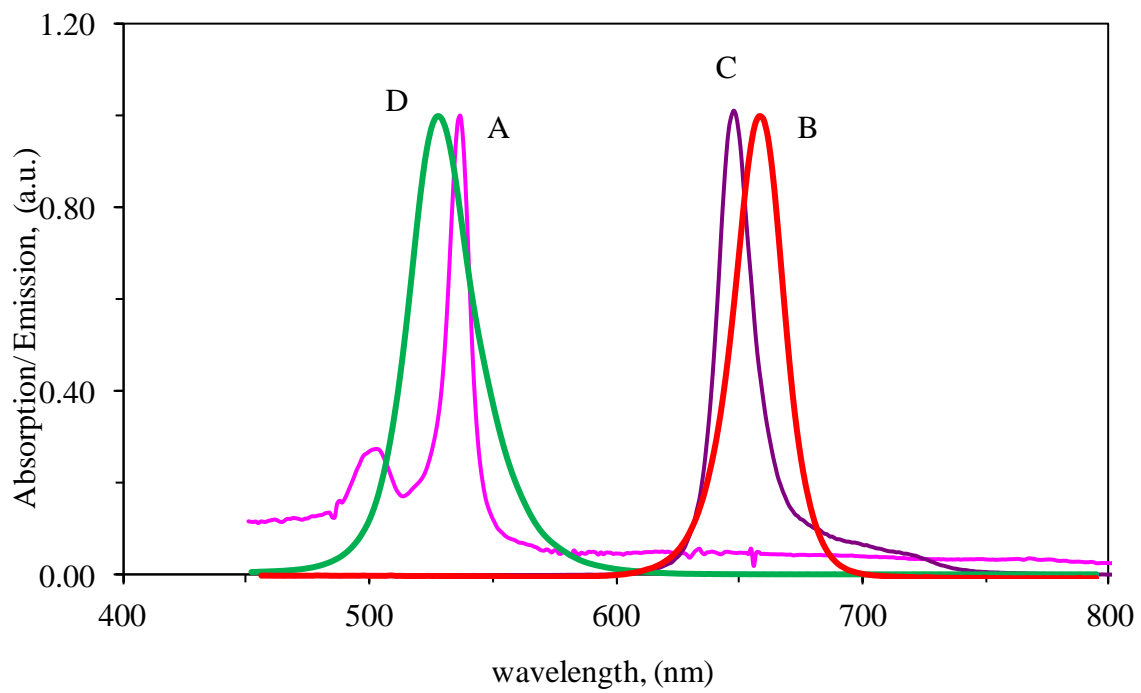


Figure 3

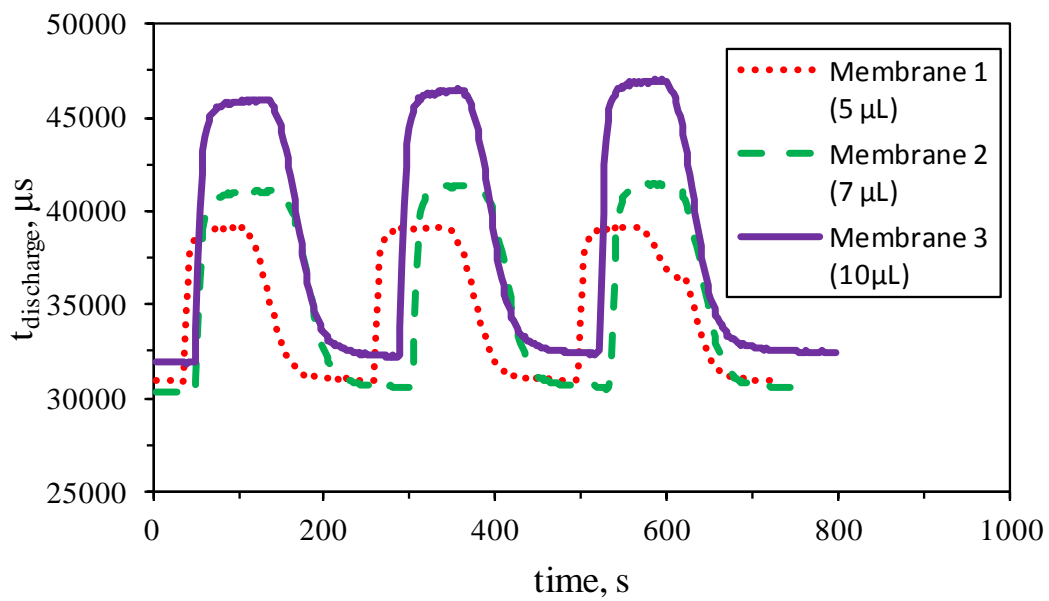


Figure 4

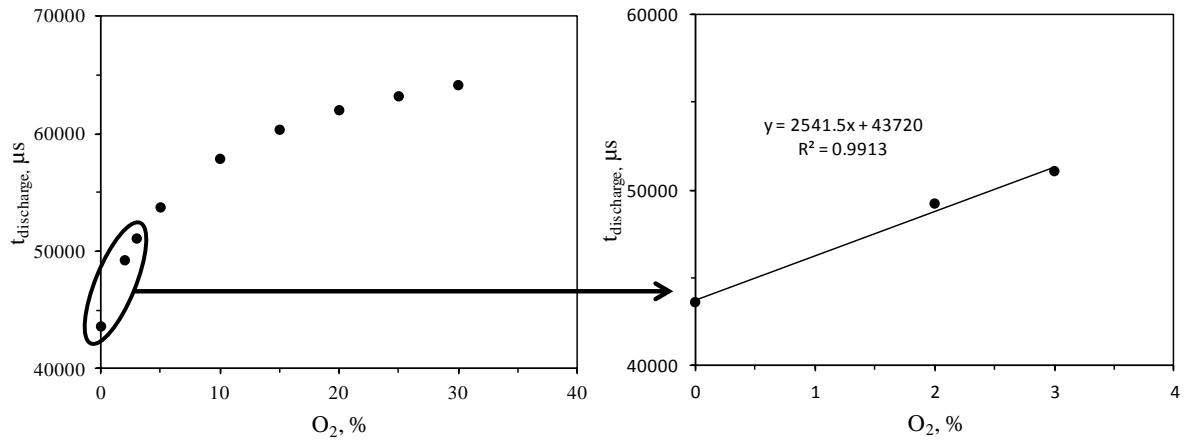


Figure 5

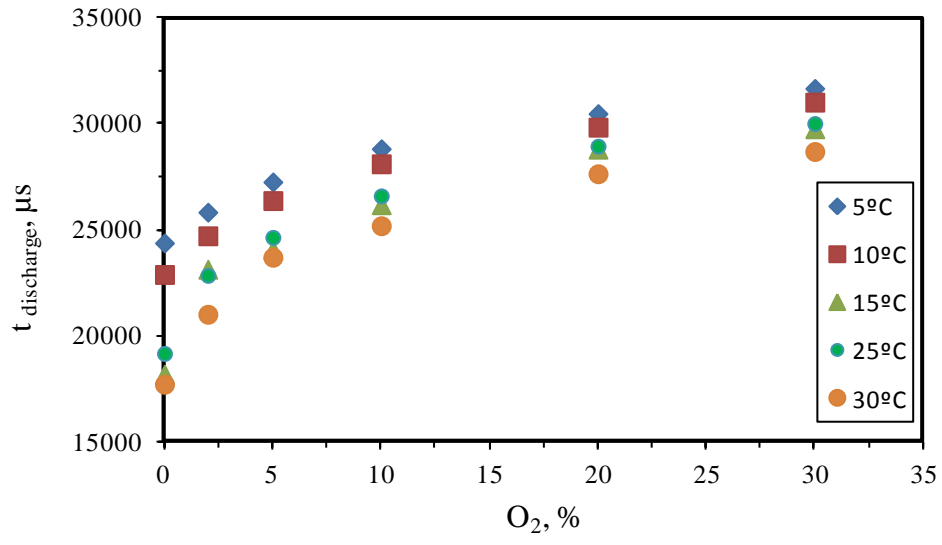


Figure 6